The Structure of Monododecyl Pentaethylene Glycol Monolayers with and without Added Dodecane at the Air/Solution Interface: A Neutron Reflection Study

J. R. Lu, Z. X. Li, and R. K. Thomas*

Physical and Theoretical Chemistry Laboratory, South Parks Road, Oxford OX1 3QZ, U.K.

B. P. Binks, D. Crichton, P. D. I. Fletcher, and J. R. McNab

School of Chemistry, University of Hull, Hull, HU6 7RX, U.K.

J. Penfold

ISIS, DRAL, Chilton, Didcot, Oxon, OX11 0QX

Received: October 13, 1997; In Final Form: March 10, 1998

Neutron reflectometry and surface tensiometry have been used to study the composition and structure of a mixed monolayer of dodecane and the nonionic surfactant pentaethylene glycol monododecyl ether ($C_{12}E_5$) and the structure of the $C_{12}E_5$ on its own at the surface of aqueous solutions of $C_{12}E_5$. Partially labeling of the surfactant with deuterium gave the surface normal distributions of the ethylene glycol and hydrocarbon chains of the surfactant and of the water, and these results are compared with those from other members of the $C_{12}E_m$ series. The $C_{12}E_5$ layer has a higher capacity for oil than that of the comparable hydrocarbon chain length cationic surfactant, dodecyl trimethylammonium bromide (C_{12}TAB), and the structure of the composite layer is also different. The separation of the centers of the surfactant chain and dodecane distributions is only 3 Å in the $C_{12}E_5$ system in comparison with 6.5 Å for C_{12}TAB. In this respect, the $C_{12}E_5$/dodecane system more closely resembles the sodium dodecyl sulfate/dodecanol system, and this is attributed to a favorable interaction between the dodecane and the ethylene glycol chain, which encourages a closer approach of the oil to the water surface. The hydrocarbon chain in the $C_{12}E_m$ series where *m* is 6 or less is tilted at about 40° away from the surface normal. Upon incorporation of dodecane into the $C_{12}E_5$ layer, the hydrocarbon chain changes to an almost perpendicular orientation.

Introduction

When small quantities of long chain liquid alkanes are placed on the surface of an aqueous surfactant solution, the equilibrium situation often consists of macroscopic oil lenses coexisting with a mixed film of surfactant and oil. In such mixed films, the oil may either be mixed with the surfactant chains, forming a film on top of the surfactant monolayer, or be present in both locations. The extent of oil penetration into surfactant monolayers at the oil/water interface is expected to be an important factor in determining the spontaneous curvature and bending elasticity of monolayers at the oil/water interface. The detailed nature of such mixed monolayers cannot be elucidated by surface tensiometry alone but requires a technique capable of determining the interfacial structure directly, such as neutron reflection. In a previous study we have used a combination of surface tensiometry and neutron reflection to investigate the composition and structure of surface films at the air−water interface formed in systems containing alkanes and the cationic alkyltrimethylammonium bromide surfactants ($C_nH_{2n+1}N(CH_3)_4$-Br abbreviated to C_nTAB).[1,2] We found partial penetration of the surfactant chains by the oil and were able to determine the individual distributions and relative positions of oil and surfactant in the direction normal to the interface. In the case of dodecane spread on C_{16}TAB, we found that the center of gravity of the oil layer coincided exactly with the outer six carbons of the surfactant C_{16} chain, some 7 Å out from the center of gravity of the C_{16} chain. The accuracy and the model independence of the geometrical information available from neutron reflection data is substantially better than from neutron small angle scattering and this information may help in obtaining a better general understanding of the interactions underlying the formation of surfactant aggregates in mixtures containing oil. Recently, using surface tensiometry and visual observation, we have studied the behavior of linear alkanes on solutions of nonionic surfactants and found that there is a transition between spreading and nonspreading behavior at an oil chainlength that depends on the structure of the surfactant.[3,4] For monododecyl pentaethylene glycol ($C_{12}E_5$), for example, this transition occurs between heptane and octane. Since the nonionic surfactants form microemulsions much more readily than the single chain cationic surfactants, it is particularly interesting to explore the surface structure in the nonionic case to see if there are any structural differences from the cationics. The C_nE_m series of surfactants has been well studied by neutron reflection (see summary results in ref 5), but no results have yet been given for $C_{12}E_5$. In this paper we present an analysis of the structure of $C_{12}E_5$ on its own and in the presence of dodecane at unit activity.

* To whom all correspondence should be addressed: Physical and Theoretical Chemistry Laboratory, South Parks Road, Oxford OX1 3QZ, U.K.

S1089-5647(97)03315-4 CCC: $15.00
Published on Web 07/08/1998

Experimental Details

The various isotopes of $C_{12}E_5$, hydrocarbon chain deuterated, ethylene glycol chain deuterated, and both chains deuterated, designated $dC_{12}hE_5$, $hC_{12}dE_5$, and $dC_{12}dE_5$, respectively, were prepared and purified as described previously.[6] The fully protonated species, $hC_{12}hE_5$, was bought from Aldrich and purified by column chromatography before use. Dodecane was obtained from Fluka (protonated) and from Merck, Sharp, and Dohme (deuterated). Polar impurities were removed from dodecane by passing over a column of alumina. Water was purified by ion exchange (Elgastat). The procedures for determining the reflectivity profiles have been fully described elsewhere.[7] The measurements were made on the reflectometers CRISP and SURF[8] at ISIS, England. The instrument was calibrated using the reflectivity profile of pure D_2O, and a flat background determined at high momentum transfer was subtracted before processing the data. The solutions were contained in Teflon troughs mounted in a sealed container. At the start of each experiment, possible surface active impurities were removed by foaming the solution in situ and removing the foam. A small quantity of dodecane containing the equilibrium monomeric concentration of nonionic surfactant was added as small liquid lenses onto the edges of the solution surface in the trough. As described in ref 3, $C_{12}E_5$ monomers distribute between water and oil and the presence of the equilibrium concentration in the added oil prevents extraction of the aqueous phase surfactant into the oil lenses. More dodecane was introduced on to filter paper mounted in a recess surrounding the trough in order to saturate the vapor. The neutron reflectivity is affected by the presence of lenses of oil on the solution but, provided that the lenses cover less than about 10% of the surface, the effect should be small. The errors arising from this problem have been discussed fully in reference.[1] All the measurements were made at ambient temperature (298 ± 2 K). Tension measurements as a function of oil vapor pressure were made using an apparatus constructed following the modified design of Cutting and Jones.[9−12] Full details of the apparatus are given in ref 13.

Results

Surface Tension. Adsorption of oil vapor causes the tension of the surfactant solution to decrease by an amount π_{oil} equal to the surface pressure of the adsorbed oil.

$$\pi_{oil} = \gamma_0 - \gamma \tag{1}$$

where γ_0 is the tension of the aqueous solution in the absence of oil and γ is the tension in the presence of the oil. The extent of oil adsorption at constant temperature and total pressure is related to the variation of tension with oil activity according to the Gibbs equation

$$-d\gamma = \sum_i \Gamma_i d\mu_i \tag{2}$$

where Γ_i and $d\mu_i$ are the surface excess concentrations and changes in chemical potential of species *i*. We assume that the addition of the oil vapor causes negligible change to the chemical potentials of the water and surfactant because of the low solubility of the alkanes in water. Thus the surface concentration of oil Γ_{oil} is related to the variation of tension with oil activity $a_{oil}(=P/P_0)$ at constant concentration of surfactant (i.e., at constant chemical potential of this species) by

$$\Gamma_{oil} = \frac{a_{oil}}{k_B T}\left(\frac{d\pi_{oil}}{da_{oil}}\right) \tag{3}$$

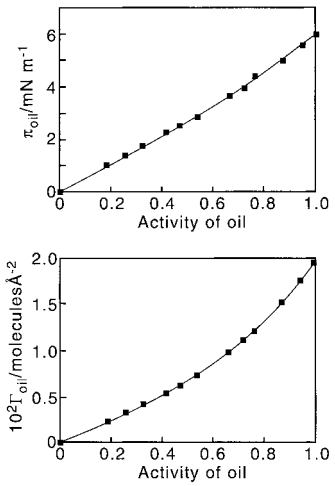

Figure 1. Variation of dodecane surface pressure (a) and surface concentration (b) with dodecane activity for adsorption on to a 1 mM aqueous solution of $C_{12}E_5$ at 298 K.

To obtain the values of Γ_{oil}, the measured surface pressure curve (π_{oil} against a_{oil}) was fitted to a polynomial function and differentiated to yield Γ_{oil} as a function of a_{oil} according to equation 3.

Figure 1a shows the variation of dodecane surface pressure with dodecane activity and Figure 1b the adsorption isotherm for 1 mM $C_{12}E_5$ solutions. The maximum adsorption corresponding to unit oil activity corresponds to an oil adsorption of approximately 1 molecule per 50 Å^2. This value is in excellent agreement with the value of 49 Å^2 obtained by neutron reflection using the lens addition method (see next section) where the oil activity is again equal to one.

Neutron Reflection. As described in earlier papers (e.g., ref 5) neutron reflection can be used to determine the surface coverage directly using measurements of a suitably deuterated surfactant dissolved in null reflecting water (NRW). NRW is a mixture of D_2O and H_2O with a composition such that its neutron scattering length (defined below) is zero. For a dilute surfactant solution, the reflected signal is then entirely from the surfactant layer from which the coverage can be obtained with almost no assumptions about the layer structure. For a detailed discussion of this point, see ref 14. The variation of coverage of $C_{12}E_5$ with concentration was determined from measurements of the neutron reflectivity of solutions of $dC_{12}hE_5$ in NRW, and the results are shown in Figure 2. Up to the critical micelle concentration (cmc) (6.4×10^{-5} M), the results are in good agreement with our own surface tension measurements. Because the activity coefficient of the surfactant cannot generally be determined above the CMC, the Gibbs equation cannot be used to determine the surface excess in this concentration range. However, there is no such problem in neutron reflection, and Figure 2 shows that the coverage reaches a plateau at the cmc which is maintained up to the highest concentration measured, 20 × cmc. The reason for including measurements at such high concentrations was that, because $C_{12}E_5$ is soluble in oil, and because in the oil spreading experiments oil drops are present at the surface, it is necessary to have an adequate reservoir of surfactant in the solution.

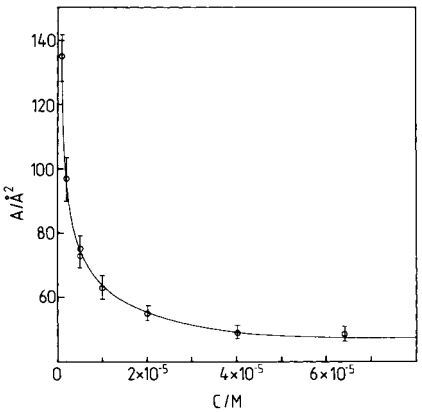

Figure 2. The area per molecule of $dC_{12}E_5$ as a function of concentration, as determined by neutron reflection.

There are two possible ways of determining the structure of a surfactant monolayer using neutron reflection. In one, the layer is divided up into uniform slabs of material, a structure for which the reflectivity can be calculated exactly,[15] and the parameters of the structure are adjusted until the calculated reflectivity matches that observed. In the second, the structure of the layer is described by analytic functions, which approximate the shapes of the distributions of the individual components and which can be Fourier transformed to give partial structure factors from which the approximate reflectivity can be calculated. Both methods rely on isotopic substitution to obtain an unambiguous description of the structure, and if enough isotopic data are available, the second method can be used to give the structure directly from the set of reflectivities. Here we mainly use the second method for determining the structure and therefore describe it in more detail.

For mixed $C_{12}E_5$/oil layers the primary features of interest are the relative positions of oil o, surfactant chain c, ethylene glycol headgroup e, the positions of all three relative to water w, and the widths of the distributions normal to the interface. In terms of these components the scattering length density, ρ, defined by

$$\rho = \sum_i b_i n_i \tag{4}$$

where b_i is the empirical scattering length of nucleus i and n_i is its number density, may be written in terms of the four components, o, c, e, and w, as

$$\rho(z) = b_o n_o(z) + b_c n_c(z) + b_e n_e(z) + b_w n_w(z) \tag{5}$$

The reflectivity in the kinematic approximation is then

$$R(\kappa) = 16\pi^2/\kappa^2 \{b_o^2 h_o + b_c^2 h_c + b_e^2 h_e + b_w^2 h_w + 2b_o b_c h_{oc} + 2b_o b_e h_{oe} + 2b_o b_w h_{ow} + 2b_c b_e h_{ce} + 2b_c b_w h_{cw} + 2b_e b_w h_{ew}\} \tag{6}$$

where the h_{ij} are the partial structure factors given by

$$h_{ii}(\kappa) = |n_i(\kappa)|^2$$

$$h_{ji} = h_{ij}(\kappa) = Re\{n_i(\kappa) n_j^*(\kappa)\} \tag{7}$$

$n_i(\kappa)$ is the one-dimensional Fourier transform of $n_i(z)$, the average number density profile of fragment i in the direction normal to the interface. Although it is simpler to express the reflectivity in terms of $h(\kappa)$, it is more convenient to do the analysis in terms of $h^{(1)}(\kappa)$, which is the equivalent transform in terms of the differential of the scattering length density. The two are related by

$$\kappa^2 h(\kappa) = h^{(1)}(\kappa) \tag{8}$$

The reflectivity given by eq 6 is approximate, but as discussed by Lu et al.,[14] it can be corrected to reduce any consequent error to a negligible level for the systems under consideration here. There are two types of partial structure factor in eq 6: the self-terms h_{ii} and the cross terms h_{ij}. The self-terms are also of two types, the first type being the surfactant and oil fragments, which can be characterized by the width σ_i and amplitude of the distribution n_i, which are both directly related to the surface coverage. The value obtained for the width depends on the function chosen to represent n_i. We shall use a Gaussian distribution for the surfactant fragments given by

$$n = n_{i0} \exp(-4z^2/\sigma_i^2) \tag{9}$$

where σ_i is the full width at $1/e$ of the maximum and which, upon Fourier transformation, gives a partial structure factor

$$h_{ii}^{(1)}(\kappa) = (\pi\sigma_i^2 n_{i0}^2/4)\kappa^2 \exp(-\kappa^2\sigma_i^2/8) \tag{10}$$

where n_{i0} is related to the surface excess by

$$\Gamma_i = \frac{1}{A} = \frac{\sigma_i n_{i0}\sqrt{\pi}}{2} \tag{11}$$

The second type of self-partial structure factor is appropriate for water. For the water distribution we use

$$n_w = n_o[^1/_2 + {}^1/_2 \tanh(z/\zeta)] \tag{12}$$

where z is the distance in the direction normal to the interface, ζ is a width parameter, and nw is the bulk number density of water in the solution. The corresponding partial structure factor is

$$h_{ww}^{(1)}(\kappa) = n_0^2(\zeta\pi\kappa/2)^2 \operatorname{cosech}^2(\zeta\pi\kappa/2) \tag{13}$$

The information about the relative positions of the distributions of each component is contained in the cross partial structure factors h_{ij}. The cross term between two distributions centered at δ_i and δ_j is

$$h_{ij}(\kappa) = Re\{n_i(\kappa) n_j^*(\kappa) \exp[-i\kappa(\delta_i - \delta_j)]\} \tag{14}$$

All distributions of the oil and of fragments of the surfactant molecule are zero at large positive and negative values of z and are therefore described by functions approximately symmetrical about their centers, whereas the solvent density is zero at large negative z but has its bulk value at large positive z and is therefore predominantly an odd function. When $n_i(z)$ and $n_j(z)$ are exactly even about their centers and $n_w(z)$ is exactly odd, equation 14 gives the following results:

$$h_{iw} = \pm(h_{ii}h_{ww})^{1/2} \sin(\kappa\delta_{iw}) \tag{15}$$

and

$$h_{ij} = \pm(h_{ii}h_{jj})^{1/2} \cos(\kappa\delta_{ij}) \tag{16}$$

The two distributions given in eqs 9 and 12 fulfill the even/odd condition exactly. We have discussed elsewhere the errors

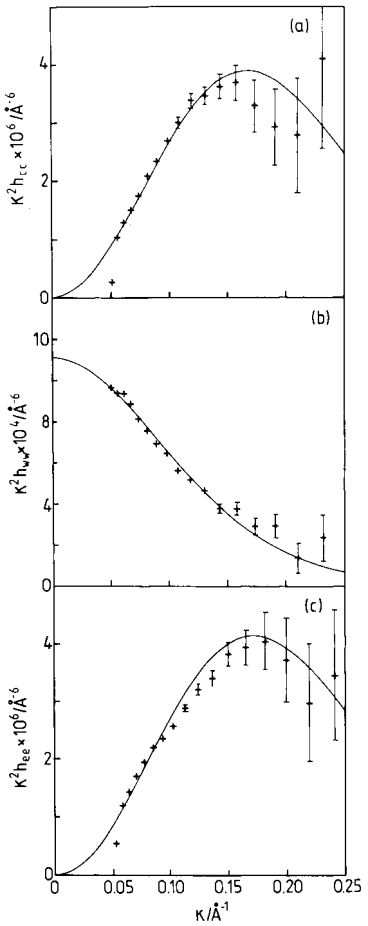

Figure 3. Self-partial structure factors for $C_{12}E_5$ at its CMC (a) h_{cc}, (b) h_{ww}, and (c) h_{ee}. The continuous lines are the best fits to the data using the parameters in Table 2.

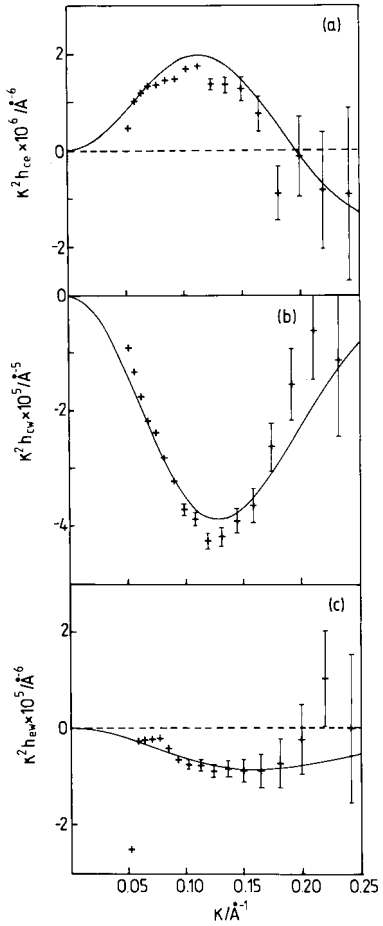

Figure 4. Cross partial structure factors for $C_{12}E_5$ at its CMC, (a) h_{ce}, (b) h_{cw}, and (c) h_{ew}. The continuous lines are the best fits to the data using the parameters in Table 2.

which might arise if any of the distribution functions are not perfectly odd or even.[16,17]

For the determination of the structure of the surfactant layer in the absence of oil, the terms involving oil (i.e., h_{io} and h_{oo}) are omitted from eq 6, leaving six partial structure factors to be determined. These were obtained from measurements of the reflectivity with the following six isotopic compositions: $dC_{12}hE_5$ in NRW and D_2O, $hC_{12}dE_5$ in NRW and D_2O, $hC_{12}hE_5$ in D_2O, and a 50:50 mixture of $dC_{12}hE_5$ and $hC_{12}dE_5$ in NRW. The last measurement is the one that is most sensitive to the separation between C_{12} and E_5. A better signal would be obtained by using the fully deuterated $dC_{12}dE_5$, but the use of the mixture gives an adequate signal and is less expensive to synthesize. After correcting the reflectivities for deviations from the kinematic approximation, the partial structure factors were obtained directly by solving the six simultaneous equations obtained from equation 6 with six sets of values of the b_i. The self-partial structure factors are shown in Figure 3 and the cross terms in Figure 4. They were fitted using eqs 10, 13, 15 and 16 with the parameters given in Table 1, and the best fits are shown as continuous lines in the two figures. A less comprehensive set of reflectivity profiles was measured at about 1/10th of the CMC, for which the results are also given in Table 1. In this case the thickness of the EO chain was not measured separately and the apparent thickness of the hydrocarbon chain, which we denote σ_c', was determined from $dC_{12}hE_5$ in NRW. Note that, because there is a small contribution to σ_c' from the protonated E_5, σ_c' is different from the true thickness of the hydrocarbon chain region σ_c.

To determine the full structure of the oil/surfactant layer in terms of the partial structure factors in eq 6 would require 10 independent measurements of reflectivity at a given composition. However, with some minor approximations, it is possible to use smaller subsets of data to extract almost the same structural information. Thus, for solutions in NRW the scattering length of the protonated ethylene glycol chain is small in comparison with the hydrocarbon layer when either chain or oil is deuterated. Thus the reflectivities of the combinations $dC_{12}hE_5$/h-dodecane (1), $hC_{12}hE_5$/d-dodecane (2), and $dC_{12}hE_5$/d-dodecane (3), all in NRW, are given respectively by

$$R_1(\kappa) \simeq \frac{16\pi^2}{\kappa^2}\{b_c^2 h_c + 2b_c b_e h_{ce}\} \tag{17}$$

$$R_2(\kappa) \simeq \frac{16\pi^2}{\kappa^2}\{b_o^2 h_o + 2b_o b_e h_{oe}\} \tag{18}$$

$$R_3(\kappa) \simeq \frac{16\pi^2}{\kappa^2}\{b_o^2 h_o + b_c^2 h_c + 2b_o b_c h_{oc} + 2b_o b_e h_{oe} + 2b_c b_e h_{ce}\} \tag{19}$$

where we have included only the largest term arising from the protonated ethylene glycol chain. These three reflectivities, shown in Figure 5, where they are also compared with the reflectivities in the absence of oil, give h_{oc} directly with almost no approximation and hence, using eq 16, δ_{oc}, the vertical distance between the centers of the oil and hydrocarbon chain

TABLE 1: Structural Parameters Obtained from Least-Squares Fitting to All the Isotopic Data at Three Concentrations Using the Kinematic Approximation

parameter	1 mM	cmc(6.4×10^{-5} M)	5×10^{-6} M
$A \pm 2$/Å^2	47	50	73
$\sigma_c \pm 2$/Å	17	17	14.5(σ'_c)
$\sigma_e \pm 2$/Å	17	16.5	
$\delta_{cw} \pm 1.5$/Å	10	10	8
$\delta_{ce} \pm 1.5$/Å	8.5	8	
$\delta_{ew} \pm 1$/Å	2	1.5	
$\xi_w \pm 2$/Å	8.5	8.5	6

distributions. This is the most interesting parameter of the composite layer. On the other hand, the widths of the chain and oil distributions, determined by approximating the terms in brackets in eqs 17 and 18 to $b_c^2 h_c$ and $b_o^2 h_o$, respectively, and then fitting eq 10 will slightly overestimate the two widths. That this inaccuracy is negligibly small is shown by the fact that our best fits to σ_c and σ_c' (σ_c' is defined at the end of the previous paragraph) gave identical values for the pure surfactant at the cmc (see Tables 1 and 2).

The reflectivities from the combinations $hC_{12}hE_5$/h-dodecane (4), $hC_{12}hE_5$/d-dodecane (5), and $dC_{12}hE_5$/h-dodecane (6), all in D_2O, and shown in Figure 6, where they are compared with the solutions in the absence of oil, are given by

$$R_4(\kappa) = (16\pi^2/\kappa^2)\{b_e^2 h_e + b_w^2 h_w + 2b_e b_w h_{ew}\} = (16\pi^2/\kappa^2)\{b'^2_w h_w\} \quad (20)$$

$$R_5(\kappa) = (16\pi^2/\kappa^2)\{b_o^2 h_o + 2b_o b_e h_{oe} + 2b_o b_w h_{ow} + b'^2_w h_w\} \quad (21)$$

$$R_6(\kappa) = (16\pi^2/\kappa^2)\{b_c^2 h_c + 2b_c b_e h_{ce} + 2b_c b_w h_{cw} + b'^2_w h_w\} \quad (22)$$

The combinations $R_5 - R_4 - R_2$ and $R_6 - R_4 - R_3$ lead to h_{ow} and h_{cw}, respectively, from which δ_{ow} and δ_{cw} can be obtained using eq 15.

The reflectivities corresponding to these six isotopic compositions were all measured at a $C_{12}E_5$ concentration of 1 mM and are shown in Figures 5 and 6 with the three key partial structure factors extracted from the data in Figure 7. In addition, we made a direct measurement of the width of the ethylene glycol chain distribution using $hC_{12}dE_6$/h-dodecane in NRW. The complete set of parameters for the mixed layer is given in Table 2. The two partial structure factors most likely to be affected by the addition of oil, h'_{cc} and h_{cw}, where the prime denotes the apparent h_{cc} determined by means of eq 17, are compared in Figure 8.

Discussion

We first discuss the structure of the $C_{12}E_5$ layer on its own. We have determined the structures of all members of the $C_{12}E_m$ series from $m = 2-6$ and also for $m = 8$ and 12.[5-6,18-20] Some of the key structural parameters at the respective cmcs are given in Table 3. The first three columns contain parameters that are accessible to classical experiments and are included for reference, although it is worth noting here that the neutron measurement of the area per molecule should generally be more precise than that determined by surface tension measurements, as we have argued elsewhere.[14] These three parameters, cmc, A_{cmc}, and γ at 10^{-4} M vary smoothly through the series, qualitatively as one might expect. The thickness of the hydrocarbon part of

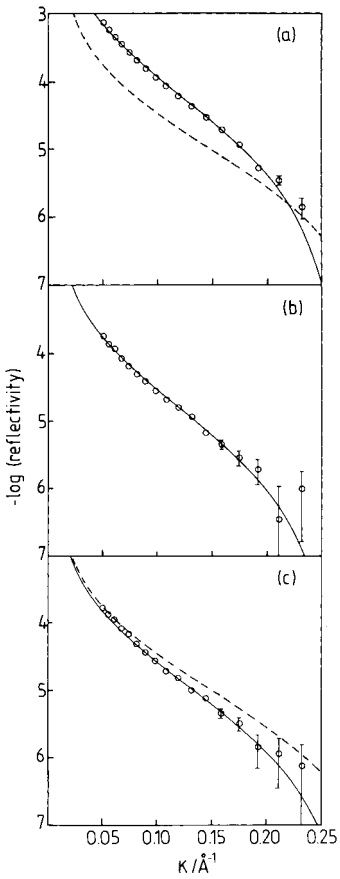

Figure 5. Reflectivities of different isotopic compositions from a dodecane layer spread on a $C_{12}E_5$ solution in null reflecting water, (a) $dC_{12}hE_5$/d-dodecane, (b) $hC_{12}hE_5$/d-dodecane, and (c) $dC_{12}hE_5$/h-dodecane. The continuous lines are the best fits to the data using the parameters in Table 2. The dashed lines are the corresponding fitted reflectivities in the absence of oil (the experimental points have been omitted for clarity). No dashed line is given for (b) because there would be no reflected signal in the absence of oil.

TABLE 2: Structural Parameters with and without Oil Layer at a Surfactant Concentration of 1 mM

parameter	1 mM	1 mM (oil)
$A \pm 2$/Å^2	47	49
$\sigma'_c \pm 2$/Å	17	20
$\sigma_e \pm 2$/Å	17	16.5
$\sigma_o \pm 2$/Å		21.5
$\delta_{co} \pm 1$/Å		3.0
$\delta_{cw} \pm 1.5$/Å	10	10.5
$\delta_{ow} \pm 1.5$/Å		13.5
$\xi_w \pm 2$/Å	8.5	8.5

the layer is constant within error at 16.5−17 Å, except for $C_{12}E_8$ and $C_{12}E_{12}$, for which it drops to 15 Å. Although it is only the last two members of the series that exhibit this lower thickness, the differences are strictly within the experimental error and this drop may not be significant. The thickness of the hydrocarbon layer includes a contribution from capillary wave roughness, for which an estimate may be made from the known surface tension, the known roughness of water,[21] and the capillary wave model for a pure liquid.[22] Thus the roughness w is given by

$$w^2 = C/\gamma \quad (23)$$

where γ is the surface tension and C is a constant obtained using a value of 2.8 Å for the roughness of water and 72 mN m^{-1} for the tension of pure water. The intrinsic thickness of the layer

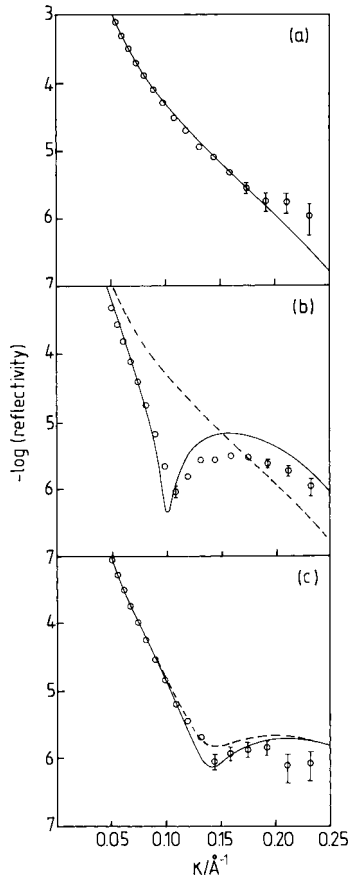

Figure 6. Reflectivities of different isotopic compositions from a dodecane layer spread on a $C_{12}E_5$ solution in D_2O, (a) $hC_{12}hE_5$/h-dodecane, (b) $hC_{12}hE_5$/d-dodecane, and (c) $dC_{12}hE_5$/h-dodecane. The continuous lines are the best fits to the data using the parameters in Table 2. The dashed lines are the corresponding reflectivities in the absence of oil (the experimental points have been omitted for clarity).

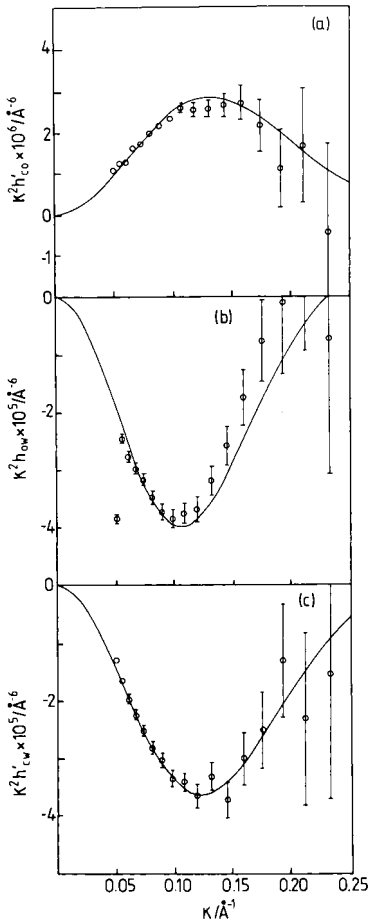

Figure 7. Cross partial structure factors from the mixed dodecane/$C_{12}E_5$ monolayer, (a) h_{co}, (b) h_{ow}, and (c) h_{cw}. The continuous lines are the best fits to the data using the parameters in Table 2.

l and the capillary wave roughness add in quadrature[14]

$$\sigma^2 = l^2 + w^2 \tag{24}$$

and hence the measured σ and calculated w can be used to calculate the 'intrinsic layer thickness' for both hydrocarbon and ethylene oxide chains, for which values are given in Table 3. The values for the hydrocarbon chain are significantly less than the length of the fully extended chain (16.7 Å),[23] which indicates that the chains are tilted away from the surface normal to about the same extent for $C_{12}E_2$ to $C_{12}E_6$. The average tilt angle can be estimated using

$$\langle \cos^2\theta \rangle = \frac{l^2}{16.7^2} \tag{25}$$

which gives a value of about 40° for the hydrocarbon chains of $C_{12}E_2$ to $C_{12}E_6$. This must be regarded as a very approximate estimate because there are a number of assumptions in the application of eq 25 as has been discussed elsewhere.[24] Although the thickness of the hydrocarbon chain region is approximately invariant down the series, the densities of the alkyl chain region of the layer relative to liquid dodecane (last column of Table 3) show a systematic decrease. These values have been calculated using the measured values of $l_c \times A$ and volumes of CH_2 and CH_3 groups of 27 and 54 Å^3, respectively.

There is a much greater variation in the length of the ethylene glycol chain in comparison with the hydrocarbon chain. The

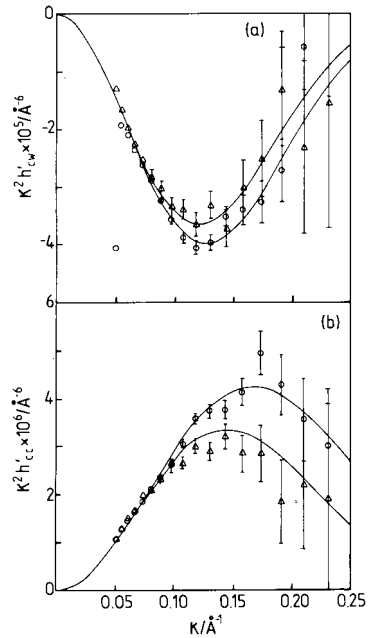

Figure 8. Comparison of partial structure factors of $C_{12}E_5$ with and without oil: (a) h_{cw} and (b) h_{cc}'.

thickness (σ) passes through a maximum at about $C_{12}E_4$ and a minimum at about $C_{12}E_6$. There appear to be two influences at work. At the low areas per molecule for the three lower members of the series the EO chain appears to be fully extended and almost completely aligned with the surface normal. Thus,

TABLE 3: Structural Parameters of $C_{12}E_m$ Layers at the CMC

	cmc ($\times 10^4$ M)	A_{cmc} ± 3/Å^2	γ at 10^{-4} M (mN m^{-1})	σ_c (± 2/Å)	l_c (± 2/Å)	σ_e (± 2/Å)	l_e (± 2/Å)	δ_{ce} (± 1/Å)	ρ/ρ_l
$C_{12}E_2$	0.3_3	33	25.5	17	13.5	12	6	8.5	0.79
$C_{12}E_3$	0.5_5	36	27.6	16.5	13	15.5	12	8.0	0.75
$C_{12}E_4$	0.6_9	44	28.6	16.5	13.5	17.5	14.5	7.5	0.59
$C_{12}E_5$	0.6_4	50	30.0	17	14	16.5	13.5	8	0.50
$C_{12}E_6$	0.8	55	33.5	16.5	13.5	15.5	12	8	0.47
$C_{12}E_8$	1.0	62	36.1	15	12	19	16.5	10.5	0.47
$C_{12}E_{12}$	1.2_5	72	38.5(CMC)	15 ± 3	12 ± 3	22 ± 4	20 ± 4	12 ± 2	0.41

the fully extended length of a single EO fragment is 3.6 Å EO length and the maximum thickness of the EO layer after removal of the capillary wave contribution would then be 7.2, 10.8, and 14.4 Å, respectively, in close agreement with the observed values of 6, 12, and 14.5 Å. However, for $C_{12}E_8$ and $C_{12}E_{12}$ the change in thickness of the EO layer is proportional to the square root of the number of EO units, which is more characteristic of polymer behavior. To some extent this pattern also occurs in the variation of the area per molecule at the CMC. Apart from the value for $C_{12}E_2$, A_{cmc} increases approximately linearly up to about $C_{12}E_6$ but then more slowly. Sarmoria and Blankschtein[11] have used the rotational isomeric state model to analyze how polymer like behavior might develop with chain length for aqueous ethylene glycol groups and concluded that polymer behavior is more or less fully developed for a free chain at $m \simeq 12$ and for an attached chain at $m \simeq 30$. The dynamic disorder in the air/water interface would create some disorder in the position of point of attachment of the EO chains and one might therefore expect fully characteristic polymer behavior at an intermediate value of m.

Table 2 compares the structure of the surfactant layer before and after addition of dodecane. The main change is in the thickness of the hydrocarbon fragment of the surfactant, which increases from 17 to 20 Å. After removal of the estimated contribution to this thickness from the capillary waves (see above) the intrinsic thickness can be seen to be changing from 14 to about 17.5 Å. Since the fully extended chain length is about 17 Å, this suggests that the chain changes from being tilted at about 40° from the surface normal in the pure surfactant layer to being approximately vertical when oil is present. Given that the vertical separation of centers of the hydrocarbon chain and the dodecane is only 3 Å, the effect of adding dodecane is approximately to double the surface density of alkyl chains, and it is clearly this interpenetration of the hydrophobic region of the surfactant by oil that causes the change in alignment of the hydrocarbon chain. The overall thickness of the dodecane, at 21.5 Å is larger than the fully extended chain length of dodecane even after allowance has been made for the capillary wave contribution. This is slightly thicker than found for dodecane layers spread on the cationic C_nTAB surfactants.[2] However, the overall coverage in the $C_{12}E_5$ layer is about 50% larger than that for the comparable CTABs. This may induce further roughening because of the lower surface tension and/or the closer packing. Interestingly, although the packing is so much greater in the $C_{12}E_5$/dodecane system, the separation between the centers of the chain and oil distributions is much less than in the C_nTAB/dodecane systems, 3 as compared with 6.5−8.5 Å. Thus the $C_{12}E_5$/oil layer is very different in character from a C_nTAB/oil layer. Indeed, the closest resemblance, both in total amount and in oil/chain separation, is the sodium dodecyl sulfate (SDS)/dodecanol system which has a similar packing density and a similar value of δ_{oc} at 3.5 Å, with an oil thickness of 19 Å.[27] In the case of the SDS/dodecanol system, one would argue that the OH group of the dodecanol would give the dodecanol some amphiphilic character and that this end of the molecule would therefore penetrate the chains to be as close to the aqueous surface as possible. The only feature of the $C_{12}E_5$ that could have an equivalent effect would be a weak attractive interaction between the EO fragment of the $C_{12}E_5$ and the dodecane, which would have an equivalent effect to the OH/water interaction in the SDS/dodecanol system. This is plausible because the $C_{12}E_5$ molecule is quite soluble in dodecane. The most direct representation of the structure obtained from a neutron reflection experiment is in terms of the number density profiles of the individual components. Almost as direct, although it requires the additional input of the estimated volume of each component is a plot of the volume fractions of the

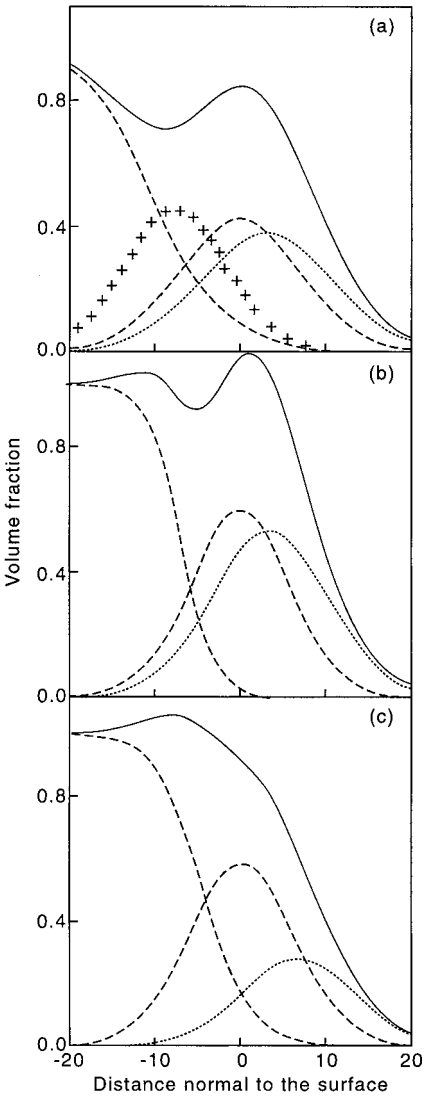

Figure 9. Volume fraction profiles for (a) $C_{12}E_5$/dodecane/water, (b) $C_{12}SO_4Na$/dodecane/water, and (c) $C_{12}TAB$/dodecane/water. The oil distribution is shown as a dotted line, the water and surfactant chains are shown as dashed lines and the total volume fraction as a continuous line. In (a) the total volume fraction does not include the ethylene glycol chain, whose distribution was not determined experimentally. The "+" represents the ethylene glycol chain distribution in the absence of oil.

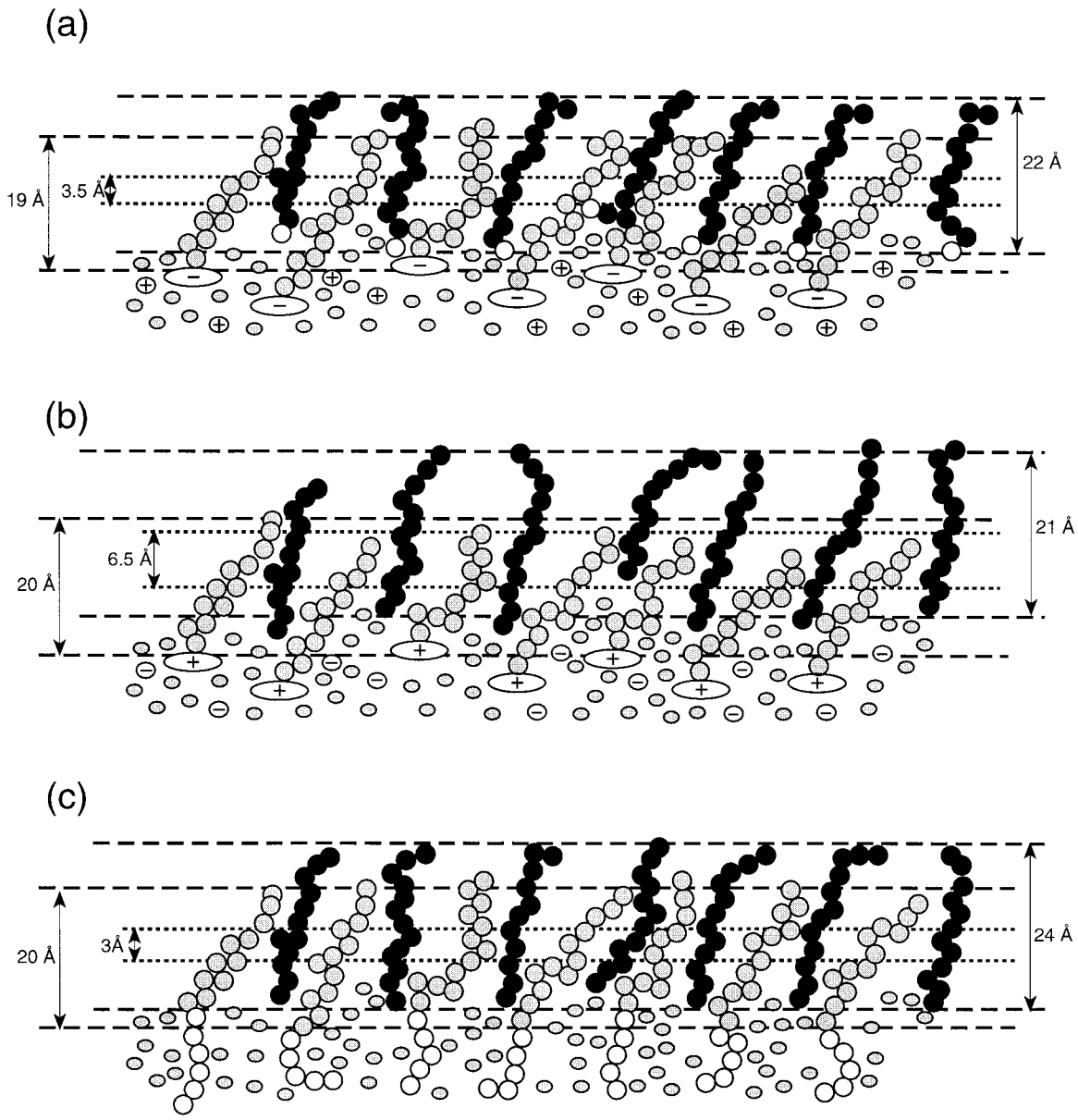

Figure 10. Schematic arrangement of three surfactant/oil systems at the air/water interface: (a) $C_{12}SO_4Na$/dodecanol/water, (b) $C_{12}TAB$/dodecane/water, and (c) $C_{12}E_5$/dodecane/water. In (a) and (c) the mean separation of hydrocarbon chain and surfactant tail, marked by dotted lines, is smaller than in (b). The surfactant chains are expected to be quite strongly tilted, given the dimensions of the layer and its expected roughness, and the oil molecules are expected to be more vertical, given the measured thickness of the layer and the assumption that the roughnesses of surfactant and oil layers are the same. The dashed lines mark the bounds of the surfactant (or surfactant chain in the case of $C_{12}E_5$) or oil layers. The structural parameters used are for uniform layer models.

fragments, which is easier to understand. These plots are given for the present $C_{12}E_5$/dodecane, $C_{12}SO_4Na$/dodecanol and $C_{12}TAB$/dodecane in Figure 9. In Figure 10 we represent the three systems schematically in a cartoon, in which it is easier to visualize the differences and similarities. The marked difference in the relative positions of surfactant and oil between the first two systems and the $C_{12}TAB$/dodecane is very clearly seen. We have not directly determined the distribution of the ethylene glycol chain in the presence of oil, and Figure 9a shows its distribution relative to the hydrocarbon chain in the absence of oil. In this position it would clearly overlap the oil distribution significantly, which gives some support to the reasoning in the previous paragraph. However, an important test of the consistency of the model distributions is that the total volume fraction does not exceed unity, which means that, within error, it must not exceed about 1:1. If the width and position of the ethylene glycol chain are assumed to be unchanged in the presence of oil this condition would be broken. To keep the volume fractions consistent, it is necessary to shift the center of the EO position to about −10 and increase the width from 16.5 to about 19 Å. In such a revised distribution of the fragments there is still significant overlap between the ethylene glycol chain and the oil.

One motivation for this study is that an understanding of the spreading of oil on surfactant layers might help toward an understanding of the oil/water interface. It is therefore interesting to compare the flat $C_{12}E_5$/oil layer with the same interface in microemulsions. Sottmann et al. examined bicontinuous microemulsions of water and dodecane stablilised by $C_{12}E_5$ using small angle neutron scattering. For a system at 41.1 °C containing equal volumes of oil and water, where the surfactant monolayer at the interface separating dodecane and water domains is disordered but has a mean curvature of zero, the area per $C_{12}E_5$ was 59−60 Å^2.[28] This is considerably higher

than the value of 49 Å^2 we observe here. They made the tentative suggestion that the difference between their values for $C_{12}E_m$ and our values for the pure surfactant layers at the air/water interface, which are all comparable with the difference of 59−60 and 47 Å^2 for $C_{12}E_5$, was caused either by the alkane film pressure or because their measurement is possibly of an undulating surface. It is clear from the present result (i.e., that the $C_{12}E_5$ area hardly changes on addition of oil) that the first explanation is not the correct one. It may also be that the comparison of the microemulsion interface with the $C_{12}E_5$/oil layer at the air/water interface is not appropriate. In this context, we note that the area of $C_{12}E_4$ adsorbed on a hydrophobic surface consisting of C_{18} hydrocarbon chains was found to be 51 Å^2, which is closer to the value of 55 Å^2 observed by Sottman et al. than the value of 44 Å^2 at the air/liquid interface.

Acknowledgment. We thank the Engineering and Physical Science Research Council for support. We also thank the University of Hull for a Graduate Teaching Assistantship to D.C. and the EPSRC for a ROPA grant to fund J.R.M.

References and Notes

(1) Lu, J. R.; Thomas, R. K.; Aveyard, R.; Binks, B. P.; Cooper, P.; Fletcher, P. D. I.; Sokolowski, A.; Penfold, J. *J. Phys. Chem.* **1992**, *96*, 10971.

(2) Lu, J. R.; Thomas, R. K.; Binks, B. P.; Fletcher, P. D. I.; Penfold, J. *J. Phys. Chem.* **1995**, *99*, 4113.

(3) Aveyard, R.; Binks, B. P.; Fletcher, P. D. I., McNab, J. R. *Langmuir* **1995**, *11*, 2515.

(4) Aveyard, R.; Binks, B. P.; Cooper, P.; Fletcher, P. D. I. *Adv. Colloid Interface Sci.* **1990**, *33*, 59.

(5) Lu, J. R.; Li, Z. X.; Thomas, R. K.; Staples, E. J.; Thompson, L.; Tucker, I.; Penfold, J. *J. Phys. Chem.* **1994**, *98*, 6559.

(6) Lu, J. R.; Hromadova, M.; Thomas, R. K.; Penfold, J. *Langmuir* **1993**, *9*, 2417.

(7) Lee, E. M.; Thomas, R. K.; Penfold, J.; Ward, R. C. *J. Phys. Chem.* **1989**, *93*, 381.

(8) Penfold, J.; Richardson, R. M.; Zarbakhsh, A.; Webster, J. R. P.; Bucknall, D. G.; Rennie, A. R.; Jones, R. A. L.; Cosgrove, T.; Thomas, R. K.; Higgins, J. S.; Fletcher, P. D. I.; Dickinson, E.; Roser, S. J.; McLure, I. A.; Hillman, R.; Richards, R. W.; Staples, E. J.; Burgess, A. N.; Blake, T. D.; White, J. W. *J. Chem. Soc., Faraday Trans.* **1997**, *93*, 3899.

(9) Cutting, C. L.; Jones, D. C. *J. Chem. Soc.* 1955, 4067.

(10) Jones, D. C.; Ottewill, R. H. *J. Chem. Soc.* 1955, 4076.

(11) Blank, M.; Ottewill, R. H. *J. Phys. Chem.* **1964**, *68*, 6.

(12) Hauxwell, F.; Ottewill, R. H. *J. Colloid Interface Sci.* **1968**, *28*, 514.

(13) Aveyard, R.; Binks, B. P.; Crichton, D.; Fletcher, P. D. I. *Langmuir*. To be submitted for publication.

(14) Lu, J. R.; Lee, E. M.; Thomas, R. K. *Acta Crystallogr*. 1996, *A52*, 11.

(15) Born, M.; Wolf, E. Principles of Optics; Regamon Press: Oxford, 1970.

(16) Simister, E. A.; Lee, E. M.; Thomas, R. K.; Penfold, J. Macromol. *Rep*. 1992, *A29*, 155.

(17) Simister, E. A.; Lee, E. M.; Thomas, R. K.; Penfold, J. *J. Phys. Chem.* **1992**, *96*, 1373.

(18) Lu, J. R.; Li, Z. X.; Su, T. J.; Thomas, R. K.; Penfold, J. *Langmuir* **1993**, *9*, 2408.

(19) Lu, J. R.; Li, Z. X.; Thomas, R. K.; Staples, E. J.; Tucker, I.; Penfold, J. *J. Phys. Chem.* **1993**, *97*, 8012.

(20) Lu, J. R.; Su, T. J.; Li, Z. X.; Thomas, R. K.; Staples, E. J.; Tucker, I.; Penfold, J. *J. Phys. Chem.* In press.

(21) Schwartz, D. K.; Schlossman, M. L.; Kawamoto, E. H.; Kellogg, G. J.; Pershan, P. S.; Ocko, B. M., Phys. Rev. A 1990, 41, 5687.

(22) Lu, J. R.; Simister, E. A.; Thomas, R. K.; Penfold, J. *J. Phys.: Condens. Matter* **1994**, *6*, A403.

(23) Tanford, C. J. *J. Phys. Chem.* **1972**, *76*, 3020.

(24) Little, D. J.; Lu, J. R.; Su, T. J.; Thomas, R. K.; Penfold, J. *Langmuir* **1995**, *11*, 1001.

(25) Takahashi, Y.; Sumita, I.; Tadokoro, H. *J. Polym. Sci.* **1973**, *11*, 2113.

(26) Sarmoria, C.; Blankschtein, D. *J. Phys. Chem.* **1992**, *96*, 1978.

(27) Lu, J. R.; Purcell, I. P.; Lee, E. M.; Simister, E. A.; Thomas, R. K.; Rennie, A. R.; Penfold, J. *J. Colloid Interface Sci.* **1995**, *174*, 441.

(28) Sottmann, T.; Strey, R.; Chen, S. H. *J. Chem. Phys*. **1997**, *106*, 6483.

(29) Fragneto, G.; Lu, J. R.; McDermott, D. C.; Thomas, R. K.; Rennie, A. R.; Gallagher, P. D.; Satija, S. K. *Langmuir* 1996, *12*, 477.